A MICROMECHANICS METHODOLOGY FOR DEFECT ASSESSMENTS IN PIPELINES

F. DOTTA and C. RUGGIERI
Dept. of Naval Architecture and Ocean Engineering,University of São Paulo, SP 05508-900, Brazil

ABSTRACT

This study extends a micromechanics approach based upon the *computational cell methodology* to model ductile crack extension of longitudinal crack-like defects in a high strength pipeline steel. Laboratory testing of an API 5L X60 pipeline steel at room temperature using standard, deep crack C(T) specimens provide the data needed to measure the crack growth resistance curve for the material. A central focus of the paper is the application of the cell methodology to predict experimentally measured burst pressures for pre-cracked pipe specimens with different crack sizes. The experimental program includes longitudinally precracked pipe specimens with 20" (508 mm) O.D. The numerical simulations demonstrate the effectiveness of the cell approach to describe crack growth response and to predict the burst pressure for the tested pipes.

1 INTRODUCTION

The accurate prediction of the failure pressure in damaged pipelines remains a key issue for the safety assessment of high pressure piping systems, including onshore and offshore facilities. Conventional failure criteria for longitudinal crack-like defects in pipelines (*e.g.*, blunt corrosion, inclusions, weld flaws, etc.) are derived based upon a simple fracture mechanics analysis for planar or crack-like flaws. Such procedures are calibrated by extensive burst testing of pipes containing machined cracks conducted on low-to-moderate strength structural steels. While these acceptance criteria for linepipe defects clearly simplify integrity analyses of in-service piping components, they essentially reflect a limit-load solution for a blunted axial crack in a pressurized vessel or pipe.

This study extends a micromechanics approach based upon the computational cell methodology to model ductile crack extension of longitudinal crack-like defects in high strength pipeline steels. Laboratory testing of an API 5L X60 steel at room temperature using standard, deep crack C(T) specimens provides the data needed to measure the crack growth resistance curve for the material. A simple scheme to calibrate material-specific parameters for the cells employs this measured R-curve. A central focus of the paper is the application of the cell methodology to predict experimentally measured burst pressures for pipe specimens with axial crack-like flaws. The experimental program includes pipe specimens with different crack depth (a) and crack size ($2c$). Plane-strain computations are conducted on detailed finite element models for the pipe specimens to describe crack extension with increased pressure. The cell model predictions of crack growth response and burst pressure predictions

are in good agreement with experimental measurements for the tested pipes. The present methodology holds significant promise as an engineering tool to simulate ductile crack growth and to predict the burst pressure of pipes and pressure vessels containing crack-like defects.

2 EXPERIMENTAL PROGRAM

To investigate the failure behavior of damaged pipelines, a series of full scale burst tests were performed on 20″ (508 mm) O.D., end-capped pipe specimens with 15.8 mm wall thickness and 3m length [1]. These experimental tests are part of a pipeline integrity program conducted by the Brazilian State Oil Company (Petrobrás) and included both internal and external longitudinal notches with different sizes measured by notch depth and notch length, $a \times 2c$: 1) 3×60 mm, 2) 7×140 mm and 3) 10×200 mm. The pipe specimens were notched along their length using an electrical discharge machine (EDM) to create the required notch shape. During the loading of the pipes, ductile crack extension was monitored by using an ultrasonic pulse technique to measure the crack growth [2].

The material is an API 5L Grade X60 pipeline steel with 483 MPa yield stress at room temperature (20 °C) and relatively low hardening properties ($\sigma_u/\sigma_{ys} \approx 1.2$). Other mechanical properties for the material includes Young's modulus, $E = 210$ GPa and Poison's ratio, $\nu = 0.3$. Laboratory testing of deep crack ($a/W = 0.5$) 0.5-T side-grooved compact tension specimens with thickness $B = 13$ mm also provided the tearing resistance curves (J vs. Δa) at room temperature (20°C) to calibrate the cell parameters for the tested pipeline steel [3]. Here a denotes the crack length and W the specimen width. The 0.5-T C(T) specimens were tested at room temperature using a direct potential (DP) method to measure the crack growth resistance for the material. After fatigue pre-cracking, the specimens were side-grooved to a depth of 1 mm on each side to promote uniform crack growth over the thickness. Figure 1 presents the experimentally measured J vs. Δa curves. The fracture tests followed the procedures of ASTM Standard Test Method for Determining J-R Curves (E1152). Experimental J-values are determined using the measured load-load line displacement records.

3 NUMERICAL MODELING OF DUCTILE CRACK GROWTH

Recent analytical efforts to model crack extension in ductile materials build upon the *computational cell* methodology which defines a single layer of void-containing, cubical cells having linear dimension D along the crack plane on which Mode I growth evolves [4, 5]. The cells have initial (smeared) void volume fraction denoted by f_0. The layer thickness (D) introduces the required length-scale over which damage occurs; elsewhere, the background material obeys the flow theory of plasticity without damage by void growth. Material outside the computational cells, the ''background" material, follows a conventional J_2 flow theory of plasticity and remains undamaged by void growth in the cells. Progressive void growth and subsequent macroscopic material softening in each cell are described with the Gurson-Tvergaard (GT) constitutive model for dilatant plasticity [6,7] given by

$$\left(\frac{\sigma_e}{\bar{\sigma}}\right)^2 + 2q_1 f \cosh\left(\frac{3q_2\sigma_m}{2\bar{\sigma}}\right) - \left(1 + q_3 f^2\right) = 0 \tag{1}$$

where σ_e denotes the effective Mises (macroscopic) stress, σ_m is the mean (macroscopic) stress, $\bar{\sigma}$ is the current flow stress of the cell matrix material and f defines the current void fraction. Factors q_1,

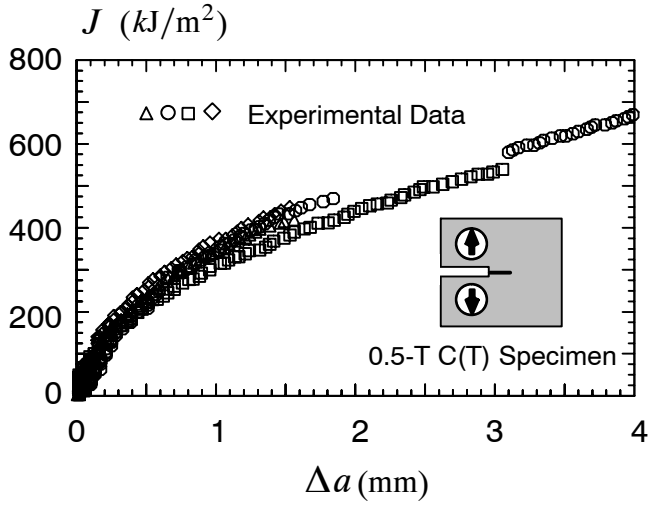

Figure 1 *Experimental R-curve for side-grooved 0.5-T C(T) specimen of API 5L-60 (20°C).*

q_2 and q_3 introduced by Tvergaard improve the model predictions for periodic arrays of cylindrical and spherical voids. Further improvement in the cell methodology [5] enables the model to create new traction free surfaces to represent physical crack extension. When f in the cell incident on the current crack tip reaches a critical value, f_E, the computational procedures remove the cell thereby advancing the crack tip in discrete increments of the cell size. The final stage of void linkup with the macroscopic crack front then occurs by reducing the remaining stresses to zero in a prescribed linear manner.

The numerical computations for the crack growth analyses reported here are generated using the research code WARP3D [8]. Nonlinear finite element analyses are performed on models for the side-grooved C(T) specimen and the longitudinally pre-cracked pipe specimen with an internal crack of 7×140 mm. Figure 2(a) shows the finite element model constructed for the plane-strain analyses of the 0.5-T C(T) specimen ($B = 13$ mm) with $a/W = 0.5$. Symmetry conditions permit modeling of only one-half of the specimen with appropriate constraints imposed on the remaining ligament. The half-symmetric model has one thickness layer of 1078 8-node, 3-D elements with plane-strain constraints imposed ($w = 0$) on each node. To simulate ductile crack extension, the finite element mesh contains a row of 130 computational cells along the remaining crack ligament ($W - a$). Plane-strain finite element analyses are also conducted on the longitudinally cracked pipes with the 7×140 mm (internal) crack. Figure 2(b) shows the finite element model constructed for this pipe specimen. The half-symmetric model has one thickness layer of 1171 8-node, 3-D elements with plane-strain constraints ($w = 0$) imposed on each node. Here, the finite element mesh contains a row of 88 computational cells along the remaining crack ligament ($t - a$).

The analyses utilize a piecewise-linear approximation of the measured engineering stress-strain curve for the API X60 steel [3] with $E = 210$ GPa and $\nu = 0.3$. The matrix material of the computational cell elements and the void-free background material are assigned these properties.

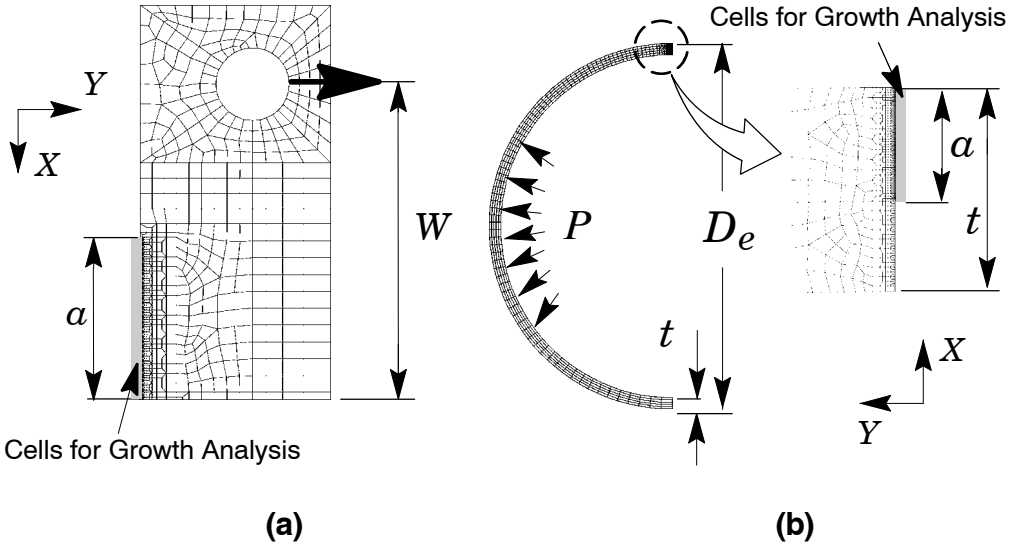

Figure 2 *Finite element models employed in the numerical analyses: a) 0.5-T C(T) specimen with a/W = 0.5; b) 20" O.D. pipe specimen with internal crack of 7 × 140 mm.*

4 BURST PRESSURE PREDICTIONS

To verify the predictive capability of the micromechanics methodology adopted in the present work, this section describes application of the cell model incorporating the Gurson-Tvergaard damage criterion to predict the measured burst pressure for the longitudinally cracked pipe with the 7 × 140 mm internal crack. The parameters governing cell response, D and f_0, are calibrated using the deep notch C(T) specimen to establish agreement between predicted and measured R-curves (see Fig. 1). The calibrated values for these parameters are then applied in similar analyses to predict ductile extension in the pre-cracked pipe specimen. Guided by similar plane-strain analyses of Xia and Shih [4] and experimental observations, the cell size is taken as $D/2 = 100\ \mu$m for the tested material. With the length scale, D, fixed for the models, the calibration process then focuses on determining a suitable value for the initial volume fraction, f_0, that produces the best fit to the measured crack growth data for the deeply cracked specimens. Figure 3 shows the measured and predicted J-Δa curves for the 0.5-T C(T) specimen. Predicted R-curves are shown for three values of the initial volume fraction, $f_0 = 0.01$, 0.008 and 0.0055. For $f_0 = 0.0055$, the predicted R-curve agrees well with the measured values for almost the entire crack extension range; for $\Delta a \geq 2$ mm the predicted curve lies a little above the measured data. In contrast, the use of $f_0 = 0.008$ and 0.01 produces a much lower resistance curve relative to the measured data. Consequently, the initial volume fraction $f_0 = 0.0055$ is thus taken as the calibrated (plane-strain) value for the API 5L-X60 steel used in the study.

These calibrated cell parameters are now employed to predict the burst pressure for these pipe specimens using the plane-strain analysis of the pipe specimen. Figure 4 shows the predicted and measured ductile crack extension with internal pressure, P. The solid symbols in the plots represent the measured crack growth for this pipe specimen. Under increased internal pressure, the amount of crack

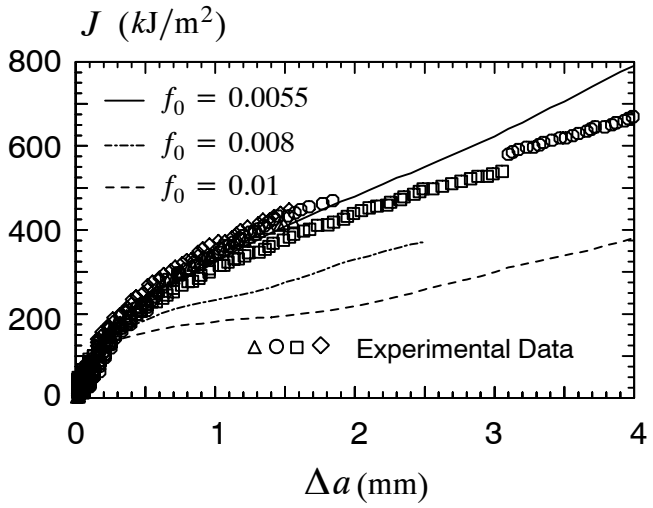

Figure 3 *Measured and predicted R-curve (plane-strain) for side-grooved 0.5-T C(T) specimen of API 5L-X60 at room temperature.*

growth increases slowly up to $P \approx 23$ MPa. The pressure value marks the beginning of very rapid ductile tearing with little increase in the applied pressure. At $P \approx 25$ MPa, the load-carrying capacity of the remaining ligament cannot keep pace with the damage accumulation in the near-tip process zone (as characterized by the large number of damaged cell elements in the numerical model) so that an instability point is reached.

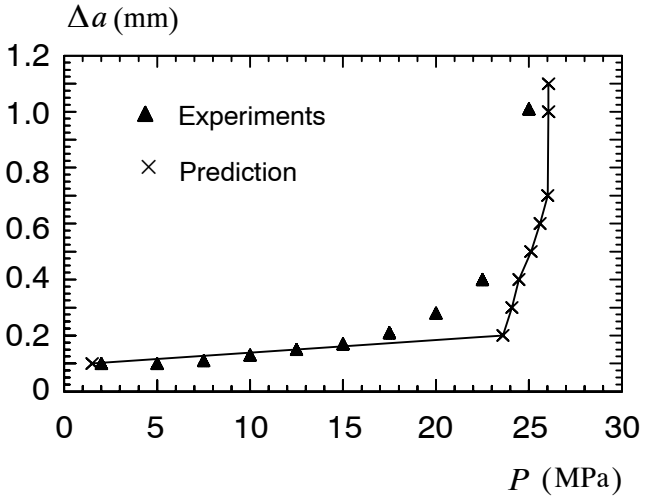

Figure 4 *Ductile crack extension for the pipe specimen with 7 × 140 mm internal crack.*

5 CONCLUDING REMARKS

This study reports on an exploratory application of the computational cell model to analyze the ductile fracture behavior of a high strength, pipeline steel (API Grade 5L X60). The plane-strain analyses reported here demonstrate the capability of the computational cell approach to simulate ductile crack growth and to correctly predict the burst pressure of the pre-cracked pipe specimen. While the present study has not explored other ranges of crack configurations, pipe diameters/wall thickness and other material properties, the results presented here represent a compelling support to the predictive capability of the cell model. More importantly, the inherent difficulty in including ductile tearing effects in burst pressure predictions within the scope of conventional procedures appears greatly reduced in the methodology presented here. Ongoing work [9] with the computational cell framework focuses on analyzing other crack configurations and modeling of ductile tearing in full 3-D setting for cracked pipelines.

Acknowledgements

This investigation is partially supported by the State of São Paulo Research Foundation (FAPESP) through Grant 03/02735-6. The authors acknowledge the Brazilian State Oil Company (Petrobrás) for making available the experimental data for the API 5L X60 pipeline steel plate and the burst pressure data. The authors also acknowledge the many useful discussions and contributions of José Claudio Guimarães Teixeira and Eduardo Hippert Jr. (CENPES-Petrobrás).

REFERENCES

[1] Petrobrás, "Burst Pressure Tests in 20" O.D. API Grade 5L X60 Pipelines," *Private Report*, 2002 (in Portuguese).

[2] Petrobrás, "Ultrasonic Measurements in Burst Pressure Tests for a 20" O.D. API Grade 5L X60 Pipelines," *Private Report*, 2002 (in Portuguese).

[3] Silva, M. S. "Fracture Toughness and *R*-Curve Measurements for an API X60 Pipeline Steel Using a Direct Current Potential Technique." *M.Sc. Thesis*. Faculty of Engineering (COPPE), Federal University of Rio de Janeiro, 2002 (in Portuguese).

[4] Xia, L. and Shih, C. F., ''Ductile Crack Growth - I. A Numerical Study Using Computational Cells with Microstructurally-Based Length Scales," *Journal of the Mechanics and Physics of Solids*, Vol. 43, pp. 233-259, 1995.

[5] Ruggieri, C., Panontin, T. L. and Dodds, R. H., 'Numerical Modeling of Ductile Crack Growth in 3-D Using Computational Cells," *International Journal of Fracture*, Vol. 82, pp. 67-95, 1996.

[6] Gurson, A. L., ''Continuum Theory of Ductile Rupture by Void Nucleation and Growth: Part I - Yield Criteria and Flow Rules for Porous Ductile Media," *Journal of Engineering Materials and Technology*, Vol. 99, pp. 2-15, 1977.

[7] Tvergaard, V., ''Material Failure by Void Growth to Coalescence," *Advances in Applied Mechanics*, Vol. 27, pp. 83-151, 1990.

[8] Koppenhoefer, K., Gullerud, A., Ruggieri, C., Dodds, R. and Healy, B., ''WARP3D: Dynamic Nonlinear Analysis of Solids Using a Preconditioned Conjugate Gradient Software Architecture", *Structural Research Series (SRS) 596*, UILU-ENG-94-2017, University of Illinois at Urbana-Champaign, 1994.

[9] Dotta, F. and Ruggieri, C., "Structural Integrity Assessments of High Pressure Pipelines with Axial Flaws Using a Micromechanics Model", *International Journal of Pressure Vessels and Piping*. Accepted for Publication.